

## Synthesis of Vinca Alkaloids and Related Compounds. 79. An Intriguing Retro Diels–Alder Reaction<sup>1</sup>

Csaba Szántay, Jr.,<sup>\*,†</sup> István Moldvai,<sup>‡</sup> Gábor Tárkányi,<sup>†</sup> and Csaba Szántay<sup>\*,‡</sup>

Chemical Works of Gedeon Richter Ltd., Spectroscopic Research Division, H-1475 Budapest, POB. 27, Hungary, and Central Research Institute for Chemistry of the Hungarian Academy of Sciences, H-1525 Budapest, POB. 17, Hungary

Received November 29, 1995<sup>⊗</sup>

The dimerization products of criocerine (**1**) are different (**2** or **3**) depending on whether the reaction is carried out in acetic acid or trifluoroacetic acid. The highly strained product **3** rearranges spontaneously through a retro Diels–Alder reaction. All structures involved were thoroughly investigated by NMR spectroscopic methods.

### Introduction

Previously, we reported<sup>2</sup> that (–)-criocerine (**1**), which is a vincamine-type alkaloid of *Crioceras dipladeniiflorus* and which bears a tetrahydrofuran ring and enamine function in ring D, gave the dimer product **2** in 86% yield by using acetic acid for the dimerization (Scheme 1). In dimer **2** the configuration of C(19') is such that C(18) occupies the thermodynamically favored equatorial position; i.e., H-19' is  $\beta$  oriented in ring D'.

Here we report that when using trifluoroacetic acid instead of acetic acid, the novel dimer **3** was obtained in 32% yield. Interestingly, in solution **3** transformed into dimer **4** in a spontaneous retro Diels–Alder reaction. The structure determination and the geometries of **3** and **4**, as investigated primarily by NMR spectroscopy, are also discussed in some detail.

### Formation of the Dimeric Product **3**

The formation of the new tetrahydropyran ring in **3** can only be accommodated by a highly strained structure in which C(18) assumes a quasi-axial position with respect to ring D'; i.e., H-19' is in the  $\alpha$  steric orientation.

A possible reaction path **1**  $\rightarrow$  **2**  $\rightarrow$  **3** was excluded by consideration of the fact that **2**, on treatment with trifluoroacetic acid, gave only **5** in 63% yield and no amount of **3** could be detected; the configuration at C(19') was retained.

To rationalize the formation of dimer **3**, two basic questions should be examined: (i) Why do the products differ when trifluoroacetic acid is used instead of acetic acid, and (ii) why does the configuration of C(19') differ in **2** and **3**?

A plausible reaction sequence may be envisaged by assuming that the monoprotonated form **6** attacks enamine **1** at C(18), forming **7** and, to a small extent, the sterically congested **8** (Scheme 2). Both **7** and **8** can be N,O-diprotonated by the strong trifluoroacetic acid (but only to a negligible extent in acetic acid), and this triggers

further transformations. Thus, the further protonation of **8** gives **9**, and similarly **7** can also be protonated. However, only **9** exhibits the steric arrangement necessary for the formation of a tetrahydropyran ring which, when coming into being, freezes the less stable compound in its form **3**. At the same time **7** equilibrates back to its components, thus shifting the whole system toward **3**. The possibility of such a reverse reaction was shown in our previous report.<sup>2</sup> Note that the curly arrows in **9** do not necessarily show a synchronized electron shift; e.g., a transient formation of a carbocation at C(17) is possible.

### Spontaneous Retro Diels–Alder Reaction

Despite its highly strained structure, dimer **3** was stable enough to facilitate structure elucidation by NMR methods (see below). However, during the course of NMR investigations **3** transformed spontaneously into dimer **4**. Conversion into **4** was practically quantitative in the NMR tube in ca. 12 h in DMSO solution at 24 °C. In CDCl<sub>3</sub> the process was much slower at ambient temperature, but full conversion could be achieved in a few hours at 50 °C. The transformation **3**  $\rightarrow$  **4** is clearly a symmetry-allowed cycloreversion, i.e., a retro Diels–Alder reaction, the driving force being the relief of the congested ring system. While the Diels–Alder-type cycloaddition is widely used in the synthesis of indole alkaloids,<sup>3</sup> a spontaneous retro Diels–Alder reaction under such mild conditions is a rare phenomenon. We should like to underline the fact that after cycloreversion molecule **4** remains a single entity, and therefore an intramolecular Diels–Alder reaction seems to be favored. However, the very high activation energy needed to follow the pathway leading to the highly strained structure of **3** prevents the cyclization. We note that the possibility of other mechanisms for the **3**  $\rightarrow$  **4** transformation (e.g., a fragmentation reaction), although unlikely, cannot be excluded.

### Structure Elucidation

The structures of compounds **3**–**5** were elucidated by the concerted application of high-field one- and two-dimensional NMR methods (DQF-COSY, HSQC, HMBC, <sup>1</sup>H{<sup>1</sup>H} and <sup>13</sup>C{<sup>1</sup>H} NOE difference) and were also

\* To whom correspondence should be addressed. Tel.: 36-1-260-57-33. Fax: 36-1-260-51-18.

<sup>†</sup> Gedeon Richter Ltd., Spectroscopic Research Division.

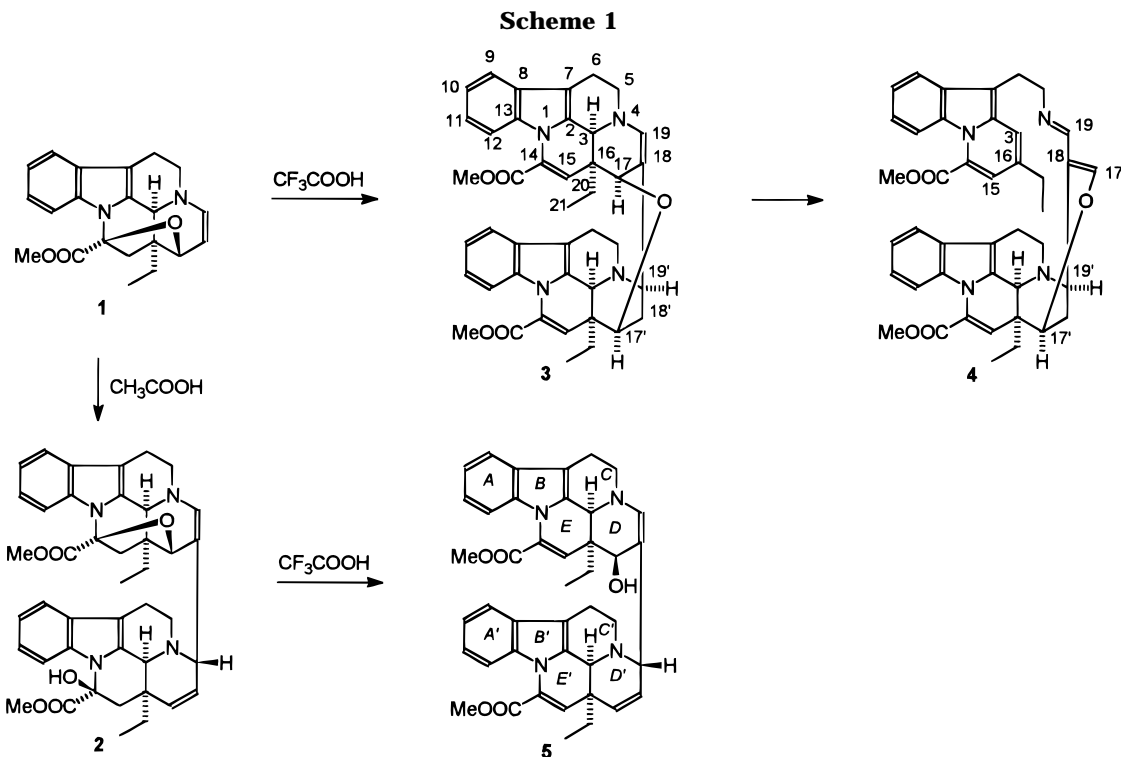
<sup>‡</sup> Central Research Institute for Chemistry.

<sup>⊗</sup> Abstract published in *Advance ACS Abstracts*, April 15, 1996.

(1) Part 78: Szabó, L.; Szántay, Cs.; Gács-Baitz, E.; Mák, M. *Tetrahedron Lett.* **1995**, *36*, 5265.

(2) Moldvai, I.; Szántay, Cs., Jr.; Tárkányi, G.; Szántay, Cs. *Tetrahedron* **1995**, *51*, 9103.

(3) Kuehne, M. E.; Brook, C. S.; Frasier, D. A.; Xu, F. *J. Org. Chem.* **1994**, *59*, 5977.



supported by MS data.  $^1\text{H}$  and  $^{13}\text{C}$  NMR data for compounds **3**–**5** are collected in Tables 1–3.

The main NMR spectroscopic properties of **1** and **2** had been reported earlier,<sup>2,4</sup> and a comparison of their NMR data with those in Tables 1–3 provides a straightforward verification for the structure of **5** with the added note that the NOE observed between H-19' and H $_{\beta}$ -6' gives experimental proof of the  $\beta$  orientation of H-19'. All interunit NOEs in **5** indicate the existence of a dominant conformation about the C(18)–C(19) bond in which H-19' and H $_{\beta}$ -6 are close in space.

Compounds **3** and **4** are both unusual in the sense that the two halves of the dimers are linked via two bonds giving highly congested geometries. The structure determination of **3** and **4** was far from straightforward, and therefore, a brief discussion of its most important aspects is given below.

**Compound 3.** MS studies indicated (see the Experimental Section) that the molecular weight of **3** formally corresponds with two units of cricoerine (**1**) minus H $_2$ O.

The  $^1\text{H}$  NMR spectrum showed two olefinic singlets at  $\delta$  5.45 and 5.61 which are directly bonded to CH carbons at  $\delta$  123.4 and 124.6, respectively. These olefinic moieties belong to separate halves of dimer **3**, which follows from the fact that one =CH proton gives NOEs into the C(16)–Et protons while the other into the C(16')–Et protons (Table 3). The C(14) and C(14') carbons (typically resonating around 80 or 90 ppm in dimers of type **2**) are shifted to ca. 130 ppm. All of this indicates that both halves of **3** contain a C(14)=C(15) double bond (cf. apovincamine<sup>5</sup>).

As compared to **1**, the aromatic regions as well as the ring-C protons and carbons, including C(3)H and C(3')H, are intact, and the relevant  $^1\text{H}$  and  $^{13}\text{C}$  signals could be readily identified. However, significant changes were found in the signals of rings D and D'. In ring D the

resonances corresponding to the C(17)H–C(18)=C(19)H subsystem are similar to those found in dimers of type **2**.<sup>2</sup> In the lower ("amine") unit an aliphatic CHCH $_2$ CH moiety could be identified. One of the CH protons was assigned to H-17' by its NOE interaction with H-15'. In light of the relevant  $^{13}\text{C}$  chemical shifts ( $\delta$  54.6,  $\delta$  35.6, and  $\delta$  60.0, respectively) this subsystem could be assigned to the C(17')HC(18')H $_2$ C(19')H moiety with C(17') assumed to be attached to an oxygen atom.

A further olefinic =CH resonates at  $\delta$  127.4 ( $^{13}\text{C}$ ) and  $\delta$  5.73 ( $^1\text{H}$ ), the latter showing a  $\approx$ 1 Hz coupling to the broadened singlet at  $\delta$  1.63.

At this point some conspicuous properties of the NMR spectra are worthy of note: (a) The relatively low-field carbon at  $\delta$  51.7 [assigned to C(17)] is directly bonded to the relatively upfield-shifted proton at  $\delta$  1.63. (b) The C(6) and C(6') carbons are found at  $\delta$  19.7 (overlapping). Assuming at this stage that C/D/E = *cis*, it is notable that C(6) and C(6') are both shifted downfield of their typical value of  $\delta \approx$ 16, as found in *cis* C/D/E vincamine-like compounds.<sup>6</sup> Such a downfield shift indicates that the characteristic C(6)  $\leftrightarrow$  C(19) and C(6')  $\leftrightarrow$  C(19')  $\gamma_{\text{gauche}}$  steric interactions (see, e.g., vincamine<sup>5,6</sup>) have both diminished; this is typical for the enamine structure found in **1** where N(4) departs from its usual pyramidal arrangement.<sup>4</sup> However, it is clear from the number of CH and CH $_2$  carbons that only one enamine moiety is present (upper half in **3**); therefore, we must assume that the unusual  $\delta$  19.7 ppm chemical shift of C(6') arises from steric factors which force N(4') to adopt a more planar geometry. (c) In one of the ethyl groups one methylene proton is very strongly shielded ( $\delta$  –0.66).

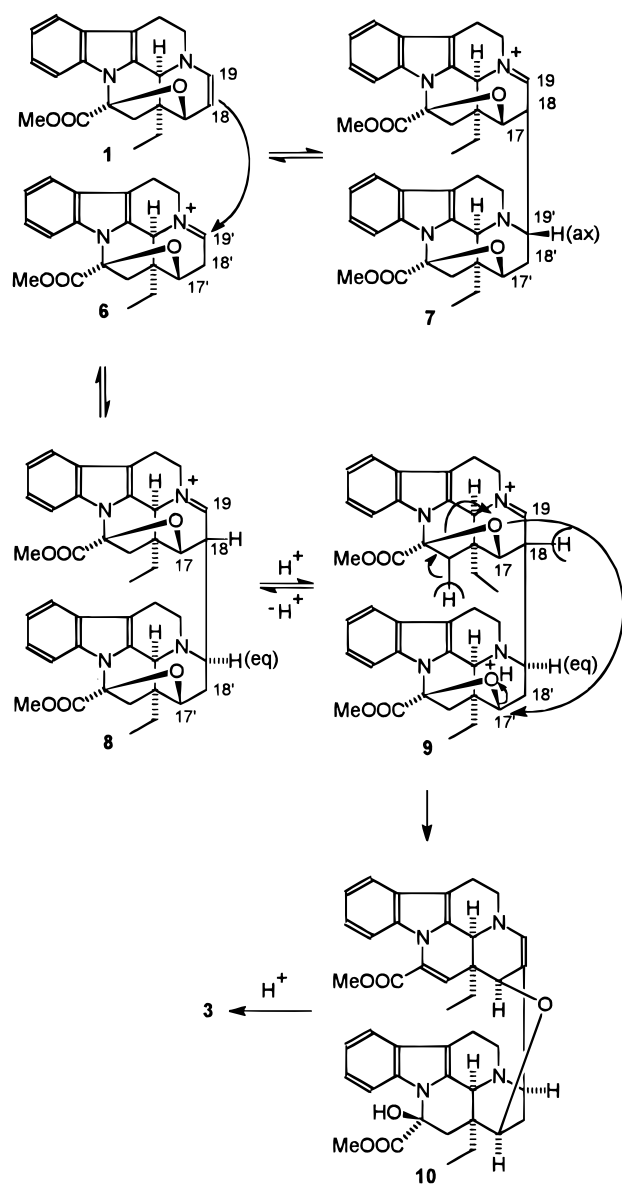
In addition to the above pieces of information, extensive use was made of the measured  $^1\text{H}\{^1\text{H}\}$  NOEs (Table 3). This led to **3** being the only structure in full agreement with the given signal assignments and measured scalar and dipolar connectivities, as well as the observed steric and anisotropic effects.

(4) (a) Moldvai, I.; Szántay, Cs., Jr.; Szántay, Cs. *Synth. Commun.* **1991**, *21*, 965. (b) Moldvai, I.; Szántay, Cs., Jr.; Szántay, Cs. *Synth. Commun.* **1992**, *22*, 509.

(5) Moldvai, I.; Szántay, Cs., Jr.; Rissanen, K.; Szántay, Cs. *Tetrahedron* **1992**, *48*, 4999 and references therein.

(6) Bombardelli, E.; Bonati, A.; Gabetta, B.; Martinelli, M.; Mustich, G.; Danieli, B. *Fitoterapia* **1975**, *46*, 51.

Scheme 2



The stereostructures of the two halves of **3** are denoted in Figure 1. Clearly, in the "amine" half (Figure 1b) H-19' and H-17' must both be equatorial, which is consistent with the relatively small vicinal scalar couplings ( $^3J < 3$  Hz) of the ring-D' protons. In addition to the intraunit NOEs, the measured interunit NOE connectivities (H-17-H $_{\beta}$ -6', H-19-H-19', H $_x$ -20-H-9', H $_x$ -20-H $_{\beta}$ -6') also confirm this stereostructure.

The above noted unique spectral features of **3** are now rationalized as follows: (a) H-17 is within the shielding zone of the indole moiety of the "amine" half (Figure 1b) which explains the apparent discrepancy between the relevant  $^1\text{H}$  and  $^{13}\text{C}$  chemical shifts for C(17)H. (b) In the "amine" unit the steric compression between the eclipsing tetrahydropyranyl ring and the indole group pushes N(4') away from its pyramidal structure (Figure 1b) and this causes a downfield shift of C(6'). (c) The irradiation of H $_3$ -21 gave significant NOEs into H-3 and H-15, but no NOE was observed on H-17 (Table 3). This indicates that the C(16)-ethyl exists predominantly in an "inward" conformation; i.e., C(21) and C(17) are anti-periplanar (Figure 1a). (Other staggered conformers involve severe inter- or intraunit steric strains). Thus, H $_y$ -20 falls into the shielding zone of the double-bond in ring E' (Figure 1b) and also receives a van der Waals

Table 1.  $^1\text{H}$  Chemical Shifts and Selected Coupling Constants for Compounds **3**–**5** (500 MHz,  $\text{CDCl}_3$ , 30 °C)

proton	<b>3</b>	<b>4</b>	<b>5</b>
3	3.99 (s) <sup>a</sup>	7.46 (s)	4.39 (s) <sup>a</sup>
5 $\alpha$ <sup>b</sup>	3.16 (ddd)	3.66 (m) <sup>c</sup>	3.43 (m)
5 $\beta$ <sup>b</sup>	3.48 (dd)	3.77 (m) <sup>c</sup>	3.66 (dd)
6 $\alpha$ <sup>b</sup>	2.48 (m)	3.30–3.43 (m)	2.76 (m)
6 $\beta$ <sup>b</sup>	2.78 (m)	3.30–3.43 (m)	2.84 (m)
9	7.33 (d)	7.83 (d)	7.43 (d)
10	7.04 (dd)	7.35 (dd)	7.08–7.15 (m)
11	7.06 (dd)	7.24 (dd)	7.08–7.15 (m)
12	7.16 (d)	7.75 (d)	7.33 (d)
15	5.45 (s)	6.82 (d)	6.22 (s)
17	1.63 (s) <sup>a</sup>	5.53 <sup>d</sup>	3.69 (d)
19	5.73 (d) ( $J_{19,17} \approx 1$ Hz)	6.95 <sup>d</sup>	5.92 (s)
20x	0.62 (dq)	2.64 (q)	1.56 (q)
20y	-0.66 (dq)	2.64 (q)	1.56 (q)
21	0.37 (t)	1.31 (t)	1.04 (t)
OMe	3.91 (s)	4.01 (s)	3.96 (s)
3'	4.40 (s) <sup>a</sup>	4.20 (s) <sup>a</sup>	4.11 (s) <sup>a</sup>
5' $\alpha$ <sup>b</sup>	3.40–3.51 (m)	3.19 (m)	2.73 (m)
5' $\beta$ <sup>b</sup>	3.40–3.51 (m)	3.50 (m)	3.31 (dd)
6' $\alpha$ <sup>b</sup>	2.45 (m)	1.78 (m)	2.46 (dd)
6' $\beta$ <sup>b</sup>	3.06 (m)	2.54 (m)	3.08 (m)
9'	7.36 (d)	6.88 (d)	7.43 (d)
10'	7.10 (dd)	6.95 (dd)	7.08–7.15 (m)
11'	7.16 (dd)	7.02 (dd)	7.08–7.15 (m)
12'	7.32 (d)	7.02 (d)	7.17 (d)
15'	5.61 (s)	5.79 (s)	5.99 (s)
17'	2.51 (t)	3.21 (s) <sup>e</sup>	5.42 (dd)
18' $\alpha$	2.02 (dt) ( $J_{17',18'\alpha,\beta} \approx 3.0$ Hz)	2.27 (d) <sup>e</sup> ( $J_{17',18'\alpha,\beta} < 3$ Hz)	5.19 (dd)
18' $\beta$	0.95 (dt) ( $J_{18'\alpha,18'\beta} = 12$ Hz)	1.32 (d) <sup>e</sup> ( $J_{18'\alpha,18'\beta} = 12$ Hz)	
19'	3.30 (t) ( $J_{19',18'\alpha,\beta} \approx 3.3$ Hz)	4.22 (s) <sup>e</sup> ( $J_{19',18'\alpha,\beta} < 3$ Hz)	3.49 (t)
20'x	1.91 (dq)	1.93 (dq)	1.69 (dq) <sup>c</sup>
20'y	1.49 (dq)	1.71 (dq)	1.76 (dq) <sup>c</sup>
21'	0.89 (t)	1.00 (t)	0.93 (t)
OMe'	4.02 (s)	3.93 (s)	3.92 (s)
OH			3.71 s

<sup>a</sup>Slightly broadened by long-range couplings. <sup>b</sup>The stereopositions  $\alpha$  and  $\beta$  are denoted relative to the plane formally defined by the two-dimensional representation of **3**–**5** as depicted in Scheme 1. <sup>c</sup>Interchangeable assignments. <sup>d,e</sup>Substantially (d) or slightly (e) broadened by chemical exchange (see text).

effect from the oxygen atom in the tetrahydropyranyl ring; this explains the highly shielded nature of H $_y$ -20 ( $\delta$  -0.66).

For the sake of comparison we note that on irradiating H $_3$ -21' NOEs were observed on H-15', H-3', and H-17', but not on H $_{\alpha}$ -18'. In this case the contribution of the conformer in which C(21) and C(15) are antiparallel is negligible, but the two other staggered conformations are both significantly populated.

**Compound 4.** The fully converted compound **4** retained the molecular weight of **3**. In the NMR spectra a set of signals could be properly assigned to the lower unit by assuming that the latter had remained intact with respect to **3**. The relevant resonances more or less accord with those of the "amine" unit in **3**. However, in the set of signals corresponding to the upper unit drastic changes took place relative to the "enamine" half of **3**. The aliphatic C(3)H, C(16), and C(17)H resonances moved into the olefinic/aromatic region. Among these two low-field CH protons (subsequently assigned to H-15 and H-3) are scalar-coupled protons ( $\approx 1$  Hz), but they show no NOE connection. The C(6) and C(5) signals both moved significantly downfield within the aliphatic range; the  $^{13}\text{C}$  resonance of C(19)H disappeared, but a very low-field CH carbon appeared at  $\delta$  162.0. With these data in mind, and by taking into account the measured scalar coupling networks and dipolar interactions, the structure of **4** could be deduced unambiguously.

**Table 2.**  $^{13}\text{C}$  Chemical Shifts for Compounds 3–5 (125 MHz,  $\text{CDCl}_3$ , 30 °C)

carbon	3	4	5
2	132.6	135.0	132.4
3	49.9	118.3	51.0
5	51.1	61.5 <sup>a</sup>	51.1
6	19.7	26.3	20.9
7	107.9	111.5	107.6
8	129.0	129.8	128.8 <sup>b</sup>
9	117.8	118.8	117.8 <sup>c</sup>
10	119.9	122.1	120.2
11	121.5	119.7	121.9 <sup>d</sup>
12	112.2	114.3	112.9
13	134.4	129.4	134.0 <sup>e</sup>
14	131.9	129.3	132.1
15	124.6	116.0	124.7
16	42.9	134.5	42.8
17	51.7	139.5 <sup>a</sup>	66.2
18	118.5	104.0	111.1
19	127.4	162.0 <sup>a</sup>	133.4
20	30.3	28.1	28.9
21	9.4	14.1	9.0
C=O	163.5	164.6	163.7
OMe	52.4	52.6	52.4
2'	134.2	131.4	131.4
3'	52.5	51.6	54.9
5'	51.1	50.0	46.0
6'	19.7	18.5	16.2
7'	107.9	111.8	109.1
8'	130.5	128.9	129.0 <sup>b</sup>
9'	118.6	118.1	118.1 <sup>c</sup>
10'	120.8	120.0	120.4
11'	122.4	121.5	122.1 <sup>d</sup>
12'	112.3	111.5	112.5
13'	134.7	133.2	134.8 <sup>e</sup>
14'	130.9	131.4	129.0
15'	123.4	121.5	123.5
16'	44.1	43.9	39.0
17'	54.6	49.7 <sup>a</sup>	127.5
18'	35.6	25.4	127.0
19'	60.0	46.4	56.9
20'	33.6	29.4	33.1
21'	9.5	9.2	9.0
C=O'	164.1	164.2	163.6
OMe'	52.6	52.5	52.5

<sup>a</sup> Substantially broadened by chemical exchange (see text).

<sup>b–g</sup> Interchangeable assignments.

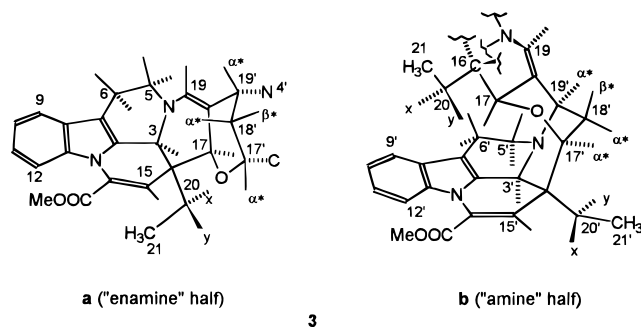


**Figure 1.** To aid clarity, unlabeled bonds denote H, and the stereoposition of some protons is labeled as  $\alpha^*$  or  $\beta^*$ ; these correspond with the relevant  $\alpha$  and  $\beta$  positions with respect to the plane formally defined by the two-dimensional representation of **3** in Scheme 1.

Again the vicinal scalar couplings of the ring-D' protons are small ( $^3J < 3$  Hz); this, in line with the observed NOEs (Table 3), indicates that the stereochemistry of ring D' is analogous to that in **3**. As opposed to **3** the H<sub>2</sub>-5 protons show NOE connection with H-9 which verifies the fact that in **4** ring C has opened up.

In **4** the ring-D' carbon resonances are all shifted 5–10 ppm upfield of their values in **3**. This is partly due to changes associated with the substituent effects of the diene moiety in the upper half of **4**. Further, as compared

to **3**, the diminished congestion of **4** allows ring D' to move closer to a chairlike geometry, which results in more pronounced  $\gamma$  steric interactions appearing on the carbons involved [this explains, e.g., the 4.6 ppm upfield shift observed on C(20')].

At room temperature some of the  $^1\text{H}$  and  $^{13}\text{C}$  signals, especially those corresponding to the diene moiety, are markedly broad, suggesting the presence of an exchange process.  $^1\text{H}$  NMR variable-temperature experiments showed, when going from +60 to –60 °C, a gradual broadening and subsequent sharpening of the signals. However, no actual splitting into further components in the (moderately) slow exchange regime was observed. This behavior is typical of a very biased exchange process which gives rise to hidden exchange partners.<sup>7</sup> The exchange process is likely to stem from the *s-cis*  $\rightleftharpoons$  *s-trans* isomerism of the diene moiety. The measured strong H-19–H-17 NOE connection indicates that the dominant isomer is the *s-trans* species. At room temperature the system is in fast exchange on the chemical shift time scale, but some signals are still close to the coalescence point which results in the observed broadening.

### Experimental Section

Melting points are uncorrected. Optical rotations were recorded in chloroform at  $25 \pm 2$  °C. Mass spectra were obtained by EI (70 eV; direct insertion) or FAB mode (NOBA matrix). NMR measurements were carried out at 30 °C in  $\text{CDCl}_3$  (500 MHz for  $^1\text{H}$  and 125 MHz for  $^{13}\text{C}$ ). Variable-temperature  $^1\text{H}$  NMR experiments were run at –60, –40, –20, 0, +30, +50, and +60 °C. Chemical shifts are given relative to  $\delta_{\text{TMS}} = 0.00$  ppm. NOE difference experiments were measured in non-degassed samples with 10 s preirradiation times. The presence of all observed  $^1\text{H}$ – $^1\text{H}$  NOEs was further verified at 300 MHz (24 °C).

**(+)-17 $\beta$ ,17' $\beta$ -Epoxy-19' $\beta$ -(18,19-didehydro-14-carbomethoxyeburnamenin-(3 $\alpha$ ,16 $\alpha$ )-18-yl)eburnamenine-(3' $\alpha$ ,16' $\alpha$ )-14'-carboxylic Acid Methyl Ester (**3**).** (–)-Cricerine (**1**) (1.0 g, 2.85 mM) was dissolved in trifluoroacetic acid (10 mL) at room temperature, and the reaction mixture was stirred for 24 h and then cooled in an ice bath. A cold concentrated aqueous ammonium hydroxide solution (20 mL) was then added to the mixture, and the precipitated crystals were filtered off, washed with cold water (50 mL), and dried to give a crude product (820 mg). The crude product was purified by using column chromatography (silica: Merck 9385; eluent: hexane + ethyl acetate 6/4). The solution was then concentrated under reduced pressure to about 5 mL and allowed to crystallize to afford **3** (285 mg, 31.7%): mp 164–166 °C; IR (KBr,  $\text{cm}^{-1}$ ) 1731, 1670, 1638, 1610, 1456, 1439, 1422, 1277, 1268, 1195, 1133, 1093, 738  $\text{cm}^{-1}$ ; Raman 1725, 1671, 1639, 1610, 1573, 1456, 1425, 1279, 1015  $\text{cm}^{-1}$ ; MS {EI}  $m/z$  682 ( $\text{M}^+$ ), 415, 386, 333, 266, 208; FAB-MS  $m/z$  683 ( $\text{MH}^+$ );  $[\alpha]_{\text{D}} +293.2$  ( $c$  0.5,  $\text{CH}_2\text{Cl}_2$ ).

**(–)-17,17' $\beta$ -Epoxy-19' $\beta$ -(3,16,17,18,19,4-hexahydro-3,4,16,17-secoeburnamenin-(3 $\alpha$ ,16 $\alpha$ )-18-yl)eburnamenine-(3' $\alpha$ ,16' $\alpha$ )-14'-carboxylic Acid Methyl Ester (**4**).** Compound **3** (136 mg, 0.2 mM) was dissolved in chloroform (5 mL), and the solution was heated at reflux for 24 h. The solvent was evaporated, and the residue was triturated with ether to give **4** as semisolid red crystals (122 mg, 90%): mp 121 °C dec; IR (KBr,  $\text{cm}^{-1}$ ) 1729, 1638, 1614, 1588, 1456, 1334, 1268, 1227, 1195, 1091, 740  $\text{cm}^{-1}$ ; Raman 1727, 1637, 1613, 1604, 1568, 1548, 1522, 1341, 1239, 1179  $\text{cm}^{-1}$ ; FAB-MS  $m/z$  683 ( $\text{MH}^+$ );  $[\alpha]_{\text{D}} -207.3$  ( $c$  0.225,  $\text{CH}_2\text{Cl}_2$ ).

**(–)-19' $\alpha$ -(18,19-Didehydro-14-carbomethoxy-17 $\beta$ -hydroxyeburnamenin-(3 $\alpha$ ,16 $\alpha$ )-18-yl)-17',18'-didehydroeburnamenine-(3' $\alpha$ ,16' $\alpha$ )-14'-carboxylic Acid Methyl Ester (**5**).** Compound **2** (200 mg, 0.285 mM) was dissolved in trifluoro-

(7) Szántay, Cs., Jr.; Demeter, Á. *J. Magn. Reson.* **1995**, *115*, 94 and references therein.

(8) Sanchez-Ferrando, F. *Magn. Reson. Chem.* **1985**, *23*, 185–191.

**Table 3.** <sup>1</sup>H NOE Connectivities<sup>a</sup> for Compounds 3–5 (500 MHz, CDCl<sub>3</sub>, 30 °C)

3		4		5	
Irradiated proton	NOE	Irradiated proton	NOE	Irradiated proton	NOE
3	<b>21</b> , 5α, 20x <sup>b</sup> , 17 <sup>b</sup>	3	20, 6α, 21, 5 <sub>d</sub> , 5 <sub>u</sub>	3	21, 5α, 20
5α	<b>5β</b> , <b>3</b> , 6α, 6β	5 <sub>d</sub> <sup>c</sup>	19, 5 <sub>u</sub> , 6, 9, 3	5α	<b>5β</b> , <b>3</b> , 6α, 6β
		5 <sub>u</sub> <sup>c</sup>	<b>19</b> , 5 <sub>d</sub> , 9, 3	5β	<b>5α</b> , <b>19</b> , 6β
		6 <sub>2</sub>	3, 9, 5 <sub>d</sub> , 5 <sub>u</sub>		
6β	<b>6α</b> , 19, 5β, 9, <u>20x</u>	9	<b>10</b> , 6, 5 <sub>u</sub> , 5 <sub>d</sub>	12	<b>11</b> , OMe
		12	<b>11</b> , OMe	15	21, 20, 17, OMe
15	21, 20y, OMe	15	20, 21, OMe	17	18', 20, 15, 21
17	20y, 20x, 6β', 3 <sup>b</sup>	17	<b>19</b>	19	<b>19'</b> , 5β, 6β, 6β', 5β', <u>5α</u> , <u>6α</u> , 20
19	<b>19'</b> , 5β, 6β, <u>5α</u> , <u>6α</u> , 6β'	20 <sub>2</sub>	21, 15, 3		
20x	<b>20y</b> , 17, 21, 3 <sup>b</sup> , 9', 6β', <u>15</u>			21	3, 20, 15, 17
20y	<b>20x</b> , 17, <b>15</b> , 21, 12'			3'	5α', 21', 20 <sub>u</sub> ', 20 <sub>d</sub> ', <u>5β'</u>
21	3, 20y, 15, 20x	3'	21', 20x', 5α', 20y'	5β'	5α', 6β', OH, 19, 19', 6β, 3'
3'	21', 20x', 5α'	6α'	6β', 5α', 9'	6α'	6β', 5α', 9', <u>19'</u>
		6β'	6α', 5β', <u>5α'</u> , 9'	6β'	6α', <b>19'</b> , 5β', 9', 19
6β'	<b>6α'</b> , 5β', 9', 20x, <u>20y</u>	15'	21', 17', 20y', 20x'	15'	<b>21'</b> , 17', 20 <sub>d</sub> ', 20 <sub>u</sub> ', OMe', <u>18'</u>
15'	21', 17', 20y', OMe'			17'	<b>18'</b> , 15', 20 <sub>d</sub> ', 21'
18α'	<b>18β'</b> , 19', 17', 20x', 20y', 3'	18α'	<b>18β'</b> , <b>19'</b> , 20x', 17', 20y'	18'	17', 19', 17, 20
18β'	<b>18α'</b> , 19', 17'			19'	<b>19</b> , 18', 6β', <u>6α'</u> , 5β'
19'	<b>19</b> , 18β', 18α', 5β'	19'	5β', 18α', 18β'	20 <sub>u</sub> '	<b>20<sub>d</sub>'</b> , 21', 3', 15'
20x'	<b>20y'</b> , 3', 21', 18α'	20x'	<b>20y'</b> , 21', 3', 18α', 15'	20 <sub>d</sub> '	<b>20<sub>u</sub>'</b> , <b>21'</b> , 17', 15', 3'
20y'	<b>20x'</b> , 17', 15', 21'	21'	15', 3', 20x', 17', 20y'		
21'	15', 3', 20x', 17', 20y'				

<sup>a</sup> Different characters are used as follows. Small: weak enhancement (NOE < 3%); normal: medium enhancement (3% < NOE < 7%); bold: strong enhancement (NOE > 7%), underlined: negative NOE. In addition, some very small long-range NOEs between relaxationally isolated protons (e.g. between H-3 and H-15) could be observed. To avoid confusion, such enhancements are not included in the table. <sup>b</sup> The small size of this enhancement is clearly due to indirect effects operating within the H-3, H<sub>x</sub>-20, H-17 three-spin system. <sup>c</sup> The subscripts "u" and "d" denote the upfield and downfield protons of the relevant geminal pair.

acetic acid (2 mL) at room temperature, and the reaction mixture was stirred for 24 h. The mixture was diluted with chloroform (100 mL), water (10 mL), and concentrated aqueous ammonium hydroxide solution (5 mL). After extraction, the organic phase was separated, washed with water (2 × 10 mL), and dried (Na<sub>2</sub>SO<sub>4</sub>). The filtrate was evaporated under reduced pressure, and the residue (190 mg) was chromatographed on silica (eluent: hexane + ethyl acetate 8/2). The solvent was evaporated under reduced pressure to yield **5** (123 mg, 63.4%). The pure residue was crystallized from methanol (5 mL): mp 215–217 °C; IR (KBr, cm<sup>-1</sup>) 3420, 1725, 1660, 1630, 1605 cm<sup>-1</sup>; FAB-MS *m/z* 683.3 (MH<sup>+</sup>, 44), 665.3 (MH – 18, 47), 416.2 (19), 333.2 (9.5), 303.1 (19.2), 208.1 (8.5); [α]<sub>D</sub> –253.6 (*c* 0.2, CHCl<sub>3</sub>).

**Acknowledgment.** The authors wish to thank the late Dr. J. Tamás and Dr. G. Czira for the mass spectra and Dr. G. Keresztúri for the IR and Raman spectra. Special thanks are due to Ms. K. Welker and Ms. I. Tóth for technical assistance.

**Supporting Information Available:** Copies of <sup>1</sup>H and <sup>13</sup>C spectra of **3–5** as well as representative examples of the variable-temperature <sup>1</sup>H NMR experiments on **4** (7 pages). This material is contained in libraries on microfiche, immediately follows this article in the microfilm version of the journal, and can be ordered from the ACS; see any current masthead page for ordering information.

JO9521110